Journal of Ginseng Research 48 (2024) 40–51

Contents lists available at ScienceDirect

Journal of Ginseng Research

journal homepage: www.sciencedirect.com/journal/journal-of-ginseng-research

Research Article

Ginsenoside 20(S)-Rg3 reduces *KIF20A* expression and promotes CDC25A proteasomal degradation in epithelial ovarian cancer

Rong Zhang [a, b, c, 1], Lei Li [d, 1], Huihui Li [a, b, 1], Hansong Bai [e], Yuping Suo [c], Ju Cui [f, **], Yingmei Wang [a, b, *]

[a] *Department of Gynecology and Obstetrics, Tianjin Medical University General Hospital, Tianjin, China*
[b] *Tianjin Key Laboratory of Female Reproductive Health and Eugenics, Tianjin Medical University General Hospital, Tianjin, China*
[c] *Department of Gynecology and Obstetrics, People's Hospital of Shanxi Province, Taiyuan, China*
[d] *Department of Radiotherapy, People's Hospital of Shanxi Province, Taiyuan, China*
[e] *Sichuan Cancer Hospital Institute, Sichuan Cancer Center, School of Medicine, University of Electronic Science and Technology of China, Chengdu, China*
[f] *The Key Laboratory of Geriatrics, Beijing Institute of Geriatrics, Institute of Geriatric Medicine, Chinese Academy of Medical Science, Beijing Hospital/ National Center of Gerontology of National Health Commission, Beijing, China*

ARTICLE INFO

Article history:
Received 16 November 2022
Received in revised form
15 June 2023
Accepted 25 June 2023
Available online 4 July 2023

Keywords:
ginsenoside Rg3
ovarian cancer
KIF20A
CDC25A
ubiquitination

ABSTRACT

Background: Ginsenoside 20(S)-Rg3 shows promising tumor-suppressive effects in ovarian cancer via inhibiting NF-κB signaling. This study aimed to explore the downstream tumor suppressive mechanisms of ginsenoside Rg3 via this signaling pathway.

Materials and methods: A systematical screening was applied to examine the expression profile of 41 kinesin family member genes in ovarian cancer. The regulatory effect of ginsenoside Rg3 on *KIF20A* expression was studied. In addition, we explored interacting proteins of KIF20A and their molecular regulations in ovarian cancer. RNA-seq data from The Cancer Genome Atlas (TCGA) was used for bioinformatic analysis. Epithelial ovarian cancer cell lines SKOV3 and A2780 were used as *in vitro* and *in vivo* cell models. Commercial human ovarian cancer tissue arrays were used for immunohistochemistry staining.

Results: *KIF20A* is a biomarker of poor prognosis among the kinesin genes. It promotes ovarian cancer cell growth *in vitro* and *in vivo*. Ginsenoside Rg3 can suppress the transcription of *KIF20A*. GST pull-down and co-immunoprecipitation (IP) assays confirmed that KIF20A physically interacts with BTRC (β-TrCP1), a substrate recognition subunit for $SCF^{\beta-TrCP}$ E3 ubiquitin ligase. *In vitro* ubiquitination and cycloheximide (CHX) chase assays showed that via interacting with BTRC, KIF20A reduces BTRC-mediated CDC25A poly-ubiquitination and enhances its stability. Ginsenoside Rg3 treatment partly abrogates *KIF20A* overexpression-induced CDC25A upregulation.

Conclusion: This study revealed a novel anti-tumor mechanism of ginsenoside Rg3. It can inhibit *KIF20A* transcription and promote CDC25A proteasomal degradation in epithelial ovarian cancer.

1. Introduction

Epithelial ovarian cancer (EOC) is a fatal malignancy in women. It acts as a "silent killer" since the symptoms are only noticeable at relatively late clinical stages (“silent”) and a high 5-year mortality rate ("killer") [1]. Most EOCs are highly sensitive to paclitaxel + platinum combination chemotherapy during initial treatment, but recurrence is inevitable due to the development of chemoresistance [2,3]. In the past decade, the application of Poly (ADP-ribose) polymerase (PARP) inhibitors significantly prolonged progression-free survival (PFS) in patients with Breast Cancer-Associated 1 and 2 (BRCA1/2) mutant ovarian cancer [4]. However, the BRCA1/2 mutation rate is around 16% to 24% in ovarian cancer patients in China [5,6]. Therefore, PARP inhibitors might not bring clinical benefits for more than 3/4 of ovarian cancer patients

* Corresponding author. Tianjin Key Laboratory of Female Reproductive Health and Eugenics, Tianjin Medical University General Hospital, Tianjin, 300052, China.
** Corresponding author.
E-mail addresses: cuiju4366@bjhmoh.cn (J. Cui), yingmeiwang@gmail.com (Y. Wang).
[1] Rong Zhang, Lei Li and Huihui Li contributed equally to this study.

https://doi.org/10.1016/j.jgr.2023.06.008

without BRCA mutations. The major mechanism of paclitaxel and platinum drugs is to promote microtubular aggregation and interfere with cell mitosis, transport and motility [7]. Therefore, an in-depth exploration of the biological characteristics of ovarian cancer cells in the process of mitosis is critical to overcome chemoresistance.

Ginsenoside 20(S)-Rg3 (ginsenoside Rg3) shows promising *in vitro* and *in vivo* tumor-suppressive effects in multiple cancers [8–10]. Ginsenoside Rg3 could induce cancer cell apoptosis [11,12], including ovarian cancer cells [13,14]. Besides, in ovarian cancer, it can inhibit hypoxia-induced epithelial-mesenchymal transition [15], indue autophagy [16], inhibit the Warburg effect [17], and suppress the expression of multiple tumor-promoting genes [17,18]. Therefore, it might be a potential candidate for adjuvant treatment. A clear understanding of the mechanisms underlying its anti-tumor effects would help promote its clinical application.

Mitosis is a highly regulated, highly ordered process. The precise progression of cytocentrosome isolation, spindle filament formation, chromosome collection, and cytoplasmic division requires the kinesin superfamily proteins (KIFs), a set of molecular motors [19]. The dysregulation of KIF proteins plays a key role in the development of human cancers [20,21]. In ovarian cancer, KIF14 expression is an independent biomarker of poor prognosis [22]. Inhibiting KIF5, an essential factor for spindle assembly, can suppress ovarian cancer growth [23]. *KIF20A* upregulation is associated with unfavorable clinical outcomes and tumor progression [24,25].

In this study, we systematically screened the KIF family member genes and confirmed *KIF20A* as a biomarker of poor prognosis and a functional tumor-promoting gene. Our bioinformatic analysis revealed that ginsenoside Rg3 might regulate *KIF20A* expression. Therefore, we further examined the effects of ginsenoside Rg3 on *KIF20A* transcription, the interacting proteins of KIF20A, and their molecular regulations in ovarian cancer.

2. Materials and methods

2.1. Bioinformatic analysis

RNA-seq data of 41 KIF family members from primary ovarian cancer cases in the cancer genome atlas (TCGA)-ovarian cancer (OV) (N = 419) and normal ovary and fallopian tube (N = 93) from the Genotype-Tissue Expression (GTEx) were extracted using the combined GTEx and TCGA dataset in UCSC Xena browser (https://xenabrowser.net/) [26]. Immunohistochemistry (IHC) staining of KIF20A expression was checked using data from the Human Protein Atlas (HPA) (https://www.proteinatlas.org/) [27]. In this database, the protein expression score is determined by manually scoring immunohistochemical data for staining intensity and the fraction of stained cells. The staining intensity is classified as negative, weak, moderate, or strong, while the fraction of stained cells is categorized as <25%, 25-75%, or >75%. Each combination of intensity and fraction is then automatically converted into a protein expression level score. A negative score indicates that the protein was not detected, while a weak score (<25%) also indicates that the protein was not detected. A weak score combined with 25-75% or 75% is classified as low. A moderate score (<25%) is classified as low, while a moderate score combined with either 25-75% or 75% is classified as medium. A strong score (<25%) is classified as medium, while a strong score combined with either 25-75% or 75% is classified as high (https://www.proteinatlas.org/about/help#4). The association between KIF20A expression and the survival outcomes of patients with primary ovarian cancer was assessed using the Kaplan-Meier plotter (http://kmplot.com/analysis/index.php?p=service&cancer=ovar), using the optimal cutoff [28].

2.2. Cell culture and treatment

Human ovarian surface epithelial (HOSE) cells and epithelial ovarian cancer cell lines (SKOV3, A2780, OV90, and OVCAR3) were cultured following the methods introduced previously [29]. Lentiviral *KIF20A* shRNAs (shKIF20A) were constructed by HanBio Technology, based on pLKO.1-puro plasmid. The following sequences were used: shKIF20A#1, 5′-CGTACACCATTCAAGGTACTA-3′, shKIF20A#2, 5′-GCTAGATGAAACAAGTCAATT-3′, shKIF20A#3, 5′- GCCACTCACAAATTTACCTTT-3'. Lentiviruses expressing myc-tagged BTRC (myc-BTRC), flag-tagged KIF20A (flag-KIF20A), and RELA (NF-κB p65) were generated based on the pLenti-puro backbone. pLenti puro HA-Ubiquitin (HA-Ub) (Plasmid #74218) was obtained from Addgene (Cambridge, MA, USA). Lentivirus for infection was produced by co-transfecting with the lentivirus packaging plasmids (pSPAX2 and pMD2.G, HanBio Technology) in 293T cells, as we previously described [30]. Cells were infected at a multiplicity of infection (MOI) of 15, with the presence of 6 μg/ml polybrene. Global protein translation inhibitor (cycloheximide, CHX) and the proteasome inhibitor MG132 were obtained from Selleck Chemicals. Ginsenoside Rg3 (purity>98%) was purchased from HerbSubstance (Chengdu, China).

2.3. Reverse transcription quantitative PCR (RT-qPCR)

In brief, cDNA was reversely transcribed using RNA samples extracted from cells and then used as the PCR assay template. Relative gene expression was normalized to *GAPDH*, by the $2^{-\Delta\Delta CT}$ method. The primers were as follows: *KIF20A*, forward: 5′-CAAGAGGCAGACTTTGCGGCTA-3′ and reverse: 5′-GCTCTGGTTCTTACGACCCACT-3'; *RELA*, forward: 5′-TGAACCGAAACTCTGGCAGCTG-3′ and reverse: 5′-CATCAGCTTGCGAAAAGGAGCC-3'; *GAPDH*, forward: 5′-GTCTCCTCTGACTTCAACAGCG-3′, and reverse, 5′-ACCACCCTGTTGCTGTAGCCAA-3'.

2.4. Western blotting

Cell samples were harvested, washed, and lysed using a lysis buffer containing protease inhibitors. After centrifugation, the supernatant was collected to determine protein concentration using a BCA kit (Beyotime). 30 μg protein samples were loaded into each lane. The following antibodies and dilutions were used, including anti-KIF20A (1:1000, 15911-1-AP, Proteintech, Wuhan, China), anti-BTRC (1:1000, 37-3400, ThermoFisher Scientific, Waltham, MA, USA), anti-Flag tag (1:5000, 66008-4-Ig, Proteintech), anti-CDC25A (1:1000, 55031-1-AP, Proteintech), anti-HA tag (1:5000, 51064-2-AP, Proteintech), anti-Myc tag (1:3000, 16286-1-AP, Proteintech), and anti-β-actin (sc-47778, Santa Cruz Biotechnology, Santa Cruz, CA, USA). HRP-conjugated secondary antibodies were used. Then, the signals were developed using the BeyoECL Star reagent (Beyotime) and a LAS-4000 imaging system (GE Healthcare, Piscataway, NJ, USA).

2.5. CCK-8 assays, colony formation, and cell cycle detection

48 h after lentiviral infections, SKOV3 and A2780 cells were seeded into 96-well plates at a density of 2,000 cells per well and were incubated for 24, 48, and 72 h. At each time point, the cell viability was measured using a CCK-8 Kit (Beyotime, Shanghai, China). 10 μl of CCK-8 reagent was added to each well and incubated for 2 h. Then, absorbance at 450 nm was measured using a microplate reader.

For colony formation assays, SKOV3 and A2780 cells with or without *KIF20A* knockdown were seeded in 6-well plates (1000 cells/per well) and cultured for 10-14 days. Then, the plates were

washed, and the colonies were fixed with 4% formaldehyde and stained with 1.0% crystal violet.

Cell cycle distribution was assessed by Propidium Iodide (PI) staining. In brief, 48 h after lentiviral infection, cells were collected and washed twice with PBS and fixed with 70% ethanol at 4°C for 1h. Then, cells were resuspended in PBS with 50 μg/mL PI and 100 μg/mL RNase A. The cells were incubated at room temperature in the dark for 30 min. Then, cell cycle distribution was detected using flow cytometry (Novocyte Advanteon, Agilent, Santa Clara, CA, USA) and analyzed using NovoExpress software (version 1.5.4, Agilent).

2.6. Nude mouse xenograft model

Female Balb/c nude mice aged 4-6 weeks were purchased from Vital River Laboratory Animal Technology (Beijing, China). All animal protocols used were approved by the Institutional Animal Care and Use Committee of Shanxi Provincial People's Hospital, China (approval no. 2022-057). All animal housing and experiments were conducted in strict accordance with the institutional Guidelines for the Care and Use of Laboratory Animals. Mice were randomly divided into four groups (n = 6 per group). Approximately 2×10^6 of A2780 or SKOV3 cells with or without *KIF20A* knockdown or SKOV3 cells with *KIF20A* overexpression were inoculated subcutaneously in the left armpit of each mouse. For the ginsenoside Rg3 treatment group, Ginsenoside Rg3 was administered at 20 mg/ kg body weight to mice 3 times per week for 4 weeks via intraperitoneal injection. Tumors were measured every 3 days with a caliper. About 4 weeks after inoculation, xenograft tumors were removed, weighed, fixed, and sectioned. IHC staining was performed to check Ki-67 expression in tumor sections.

2.7. Glutathione-S-transferase (GST) pull-down and co-immunoprecipitation (IP) assays

The genes encoding BTRC, FBXW11, and FBXW7 were subcloned in pGEX-6p-1 between the EcoRI and XhoI restriction sites. GST-fusion proteins were expressed in E. coli BL21 (DE3). In brief, the ligation mixture was transformed into competent E. coli cells and plated on LB agar plates containing ampicillin. A single colony was picked and grown in LB broth containing ampicillin. When the OD600 of the LB medium reached 0.6-0.8, protein expression was induced by adding IPTG to a final concentration of 0.1 mM and continuing to incubate for 4 h at 37°C with shaking. The cells were harvested by centrifugation at 4,000 × g for 10 min at 4°C, resuspended in lysis buffer containing protease inhibitors, and lysed by sonication. The lysates were centrifugated at 12,000 × g for 15 min at 4°C to remove cell debris. The supernatant was collected and incubated with Glutathione-Sepharose beads for 1 h at 4°C with gentle shaking. Then, the beads were washed several times with lysis buffer to remove non-specifically bound proteins. The GST-tagged proteins were eluted from the beads by adding an elution buffer. Then, GST pull-down assays were performed using Pierce GST Protein Interaction Pull-Down Kit (ThermoFisher Scientific), following the protocol of the kit. The bait GST-tagged proteins were immobilized on the pierce spin column with equilibrated glutathione agarose. The supernatant from HEK293T cells overexpressing flag-tagged KIF20A (as prey protein) was prepared and added to the pierce spin column containing the immobilized GST-tagged proteins and then incubated at 4°C for 4 h with gentle rocking. Then, the column was washed several times and the bait-prey proteins were eluted with the glutathione elution buffer. The eluted samples were subjected to western blotting assays. Co-IP assay was performed as we previously described [30], using mouse anti-BTRC (37-3400, ThermoFisher Scientific), rabbit anti-KIF20A (15911-1-AP, Proteintech), and protein A agarose (sc-2001, Santa Cruz).

2.8. Immunofluorescent staining

Immunofluorescent staining was performed following the methods introduced previously [31]. In brief, cells were grown on coverslips. After about 50% confluence, cells were fixed and permeabilized. Then, the cells were washed and incubated with primary antibody against BTRC and KIF20A (mouse anti-BTRC, 1:200, 37-3400, ThermoFisher Scientific and rabbit anti-KIF20A, 1: 200, 15911-1-AP, Proteintech) at 4 °C overnight. The CoraLite594-conjugated Goat Anti-Mouse IgG(H + L) and CoraLite488-conjugated Goat Anti-Rabbit IgG(H + L) (Proteintech) were used as the secondary antibodies. Nuclei were stained with DAPI. Immunofluorescent images were acquired using IX83 (Olympus, Tokyo, Japan).

2.9. Statistical analysis

Welch's t-test was conducted to check the statistical difference between the two groups. One-way ANOVA with post-hoc Tukey test was performed for multiple-group comparisons. Log-rank test was performed in Kaplan-Meier (K-M) survival analysis. Pearson's r or Spearman's rho values were calculated to estimate correlations. $p < 0.05$ was considered statistically significant.

3. Results

3.1. Systematic screening identifies a link between KIF20A upregulation and unfavorable prognosis of ovarian cancer

To explore dysregulated KIF genes, we extracted RNA-seq data of 41 KIF family members from primary ovarian cancer cases in TCGA-OV (N = 419) and normal ovary and fallopian tube (N = 93) from GTEx (Fig. S1A). The dysregulated genes were identified by the following criteria: serous EOC (SEOC) vs. normal ($\log_2$ fold change ≥ 2) and adj. $p < 0.05$. After the screening, 14 candidates were identified, including *KIF18B*, *KIF20A*, *KIF14*, *KIF11*, *KIF18A*, *KIF2C*, *KIF15*, *KIFC1*, *KIF1A*, *KIF23*, *KIF12*, *KIF26B*, *KIF6*, and *NEK6* (Fig. S1B). K-M survival analysis using data from the Kaplan-Meier plotter confirmed that high *KIF20A* expression was associated with significantly worse PFS (HR: 1.35, 95%CI: 1.12-1.63, $p = 0.0015$) and OS (HR: 1.25, 95%CI: 1.06-1.46, $p = 0.006$) (Fig. 1A–B). To explore KIF20A expression at the protein level, we conducted IHC staining using a commercial ovarian cancer tissue assay. Results confirmed medium to high KIF20A expression, mainly in the nucleus (Fig. 1C).

Then, we examined the IHC staining of KIF20A in the Human Protein Atlas (HPA) [27]. In the HPA, KIF20A was examined in 12 ovarian cancer tissues using two antibodies (HPA036909 and HPA036010) (Fig. S2). Medium to high expression of KIF20A was observed in most of the tumor tissues (Fig. S2). Subcellular analysis showed that KIF20A is mainly distributed in the nucleus, with minor distribution in the cytoplasm (Fig. S2, top panels, enlarged areas).

3.2. Knockdown of KIF20A impairs ovarian cancer cell proliferation in vitro

KIF20A expression in normal human ovarian surface epithelial (HOSE) cells and multiple ovarian cancer cell lines, including SKOV3, A2780, OV90, and OVCAR3, were examined. Results showed that the tumor cell lines had significantly elevated KIF20A expression at the mRNA and protein levels than HOSE cells (Fig. S3A-B). SKOV3 and A2780 were selected as representative cell lines for

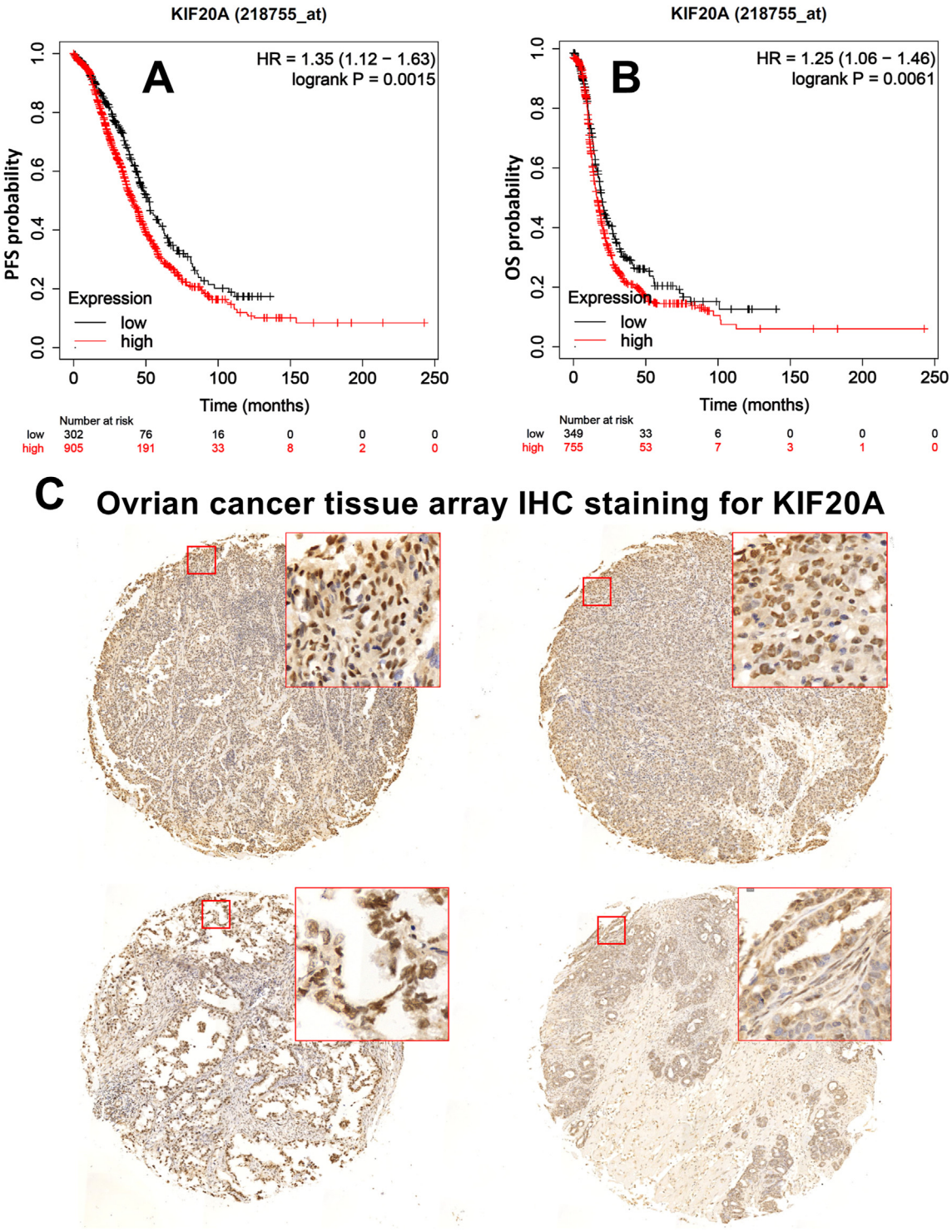

Fig. 1. Systematic screening identifies a link between *KIF20A* upregulation and unfavorable prognosis of ovarian cancer, **A-B.** K-M plotter was generated to compare the difference in PFS (C) and OS (D) between patients with high and low *KIF20A* expression with survival data from the Kaplan-Meier plotter. **C.** Representative images of KIF20A expression in commercial ovarian cancer tissue arrays. Enlarged tissue areas were provided to show the subcellular distribution of KIF20A.

further studies. These two cell lines were subjected to *KIF20A* knockdown or overexpression using lentiviruses (Fig. S1C-F). CCK-8 (Fig. 2A–B), colony formation (Fig. 2E–F), and flow cytometric analysis (Fig. 2H–J) showed that *KIF20A* knockdown significantly reduced cell viability, colony formation, cells in the S phase, and increased G1 phase arrest of SKOV3 and A2780 cells (Fig. 2E–H). In comparison, *KIF20A* overexpression significantly enhanced proliferation and cell cycle progression (Fig. 2A–J).

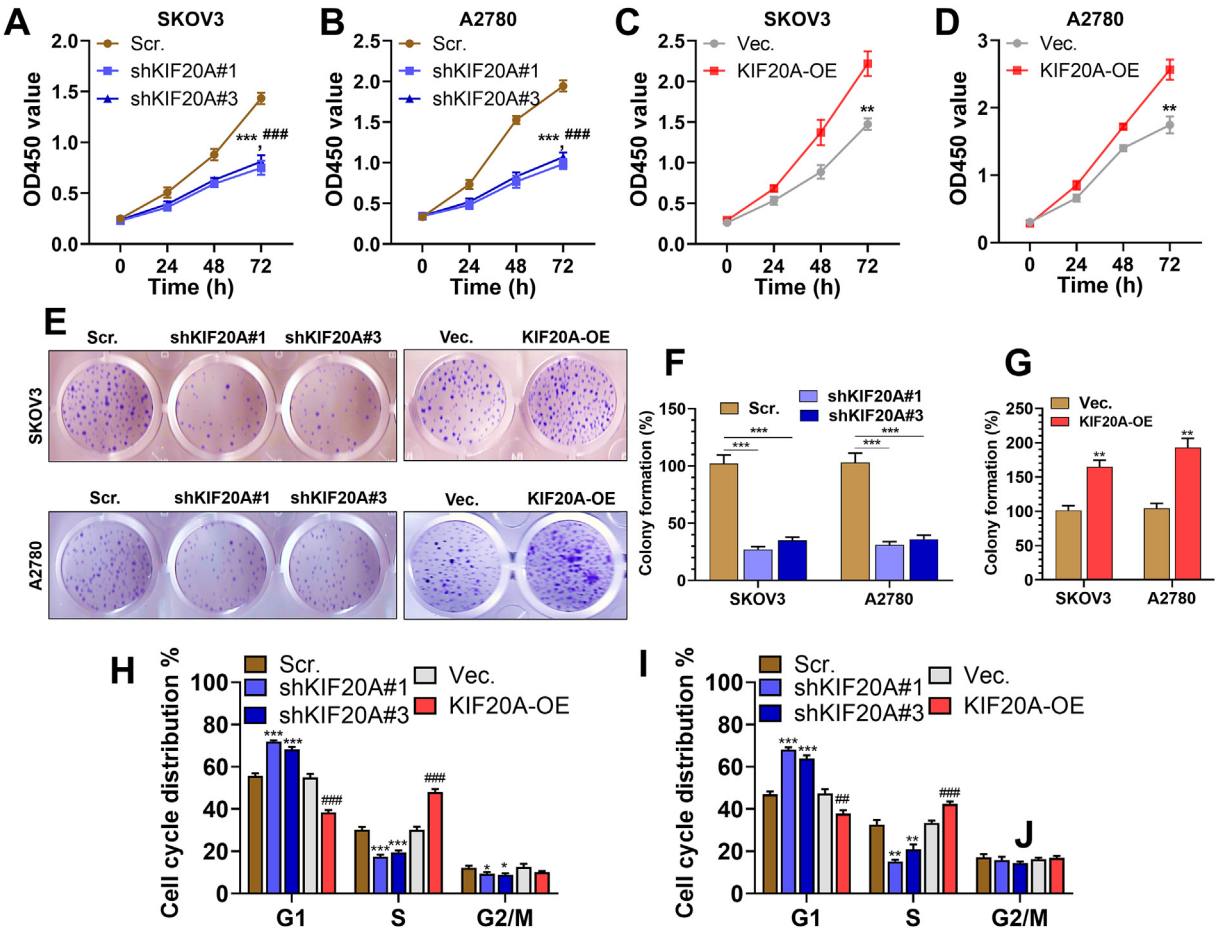

Fig. 2. Knockdown of *KIF20A* impairs ovarian cancer cell proliferation, **A-D.** CCK-8 assays showing the effects of *KIF20A* knockdown (A-B) or overexpression (C-D) on the viability of SKOV3 (A and C) and A2780 (B and D) cells. **E-I.** Colony formation (E-G) and flow cytometric analysis (H–I) were performed to show the effect of *KIF20A* knockdown or overexpression on colony formation and cell-cycle distribution of SKOV3 and A2780 cells. Data are expressed as mean ± SD. *, comparison between scramble (scr.) control and shKIF20A. # comparison between vector (vec.) and KIF20A-OE. ## and**$p < 0.01$, ### and ***$p < 0.001$.

3.3. Ginsenoside Rg3 suppresses KIF20A expression in ovarian cancer cells

By performing *KIF20A* promoter scanning, we observed high-potential binding sites of NF-κB p65/RELA (Figure S4, bold green nucleobases). Therefore, we further checked the expressional correlation between *KIF20A* and *RELA* in primary ovarian cancer cases in TCGA. Correlation analysis confirmed a moderate positive correlation (Pearson's r = 0.50) (Fig. 3A). Ginsenoside Rg3 has well-documented effects on inhibiting the activity of NF-κB p65 via suppressing its phosphorylation [32–34]. Therefore, we explored its effects on *KIF20A* expression in ovarian cancer cells. As expected, it suppressed *KIF20A* expression dose-dependently (Fig. 3B–C). To validate this finding, we overexpressed *RELA* in SKOV3 and A2780 cells (Fig. 3D–F). *RELA* overexpression was associated with increased NF-κB p65 phosphorylation (Fig. 3F–H) and increased *KIF20A* expression at the mRNA (Fig. 3D–E) and protein levels (Fig. 3F–H). Ginsenoside Rg3 treatment significantly weakened *RELA* overexpression-induced *KIF20A* upregulation (Fig. 3D–H).

3.4. KIF20A directly interacts with BTRC

To explore the potential functional regulation of KIF20A, we checked its interacting proteins using BioGRID (https://thebiogrid.org/). Only the proteins with minimum evidence ≥2 (at least two previous experimental evidence) were identified (Fig. 4A). Among the candidates, BTRC (also known as β-TrCP1) and FBXW11 (β-TrCP2) were two potential candidates (Fig. 4A). BTRC serves as the substrate recognition subunit for $SCF^{\beta-TrCP}$ E3 ubiquitin ligase, which specifically ubiquitinates phosphorylated substrates [35]. This E3 ligase exerts critical regulations on cell cycle progression and tumorigenesis by controlling the degradation of multiple essential cell cycle regulators [36].

To validate the specificity of the potential interactions, we generated recombinant pGEX-GST vectors expressing BTRC, FBXW11, and, another well-characterized F-box protein FBXW7. GST-fusion proteins were expressed in E. coli BL21 (DE3). Flag-KIF20A was expressed in 293T cells. Then, a GST pull-down assay was performed. Results showed that KIF20A exhibited a weak binding to FBXW11 and FBXW7 and a strong affinity to BTRC (Fig. 4B). The interaction between KIF20A and BTRC was also validated at the endogenous level. In the cell lysates from SKOV3 and A2780 cells, BTRC was identified in the KIF20A enriched fraction, and KIF20A was co-isolated with BTRC reciprocally (Fig. 4C–D). Immunofluorescent staining confirmed the co-localization between endogenous BTRC and KIF20A in the nucleus (Fig. 4E).

3.5. Ginsenoside Rg3 promotes CDC25A proteasomal degradation via suppressing KIF20A expression

Since we validated the interaction between KIF20A and BTRC, we hypothesized that KIF20A might exert specific regulation on the

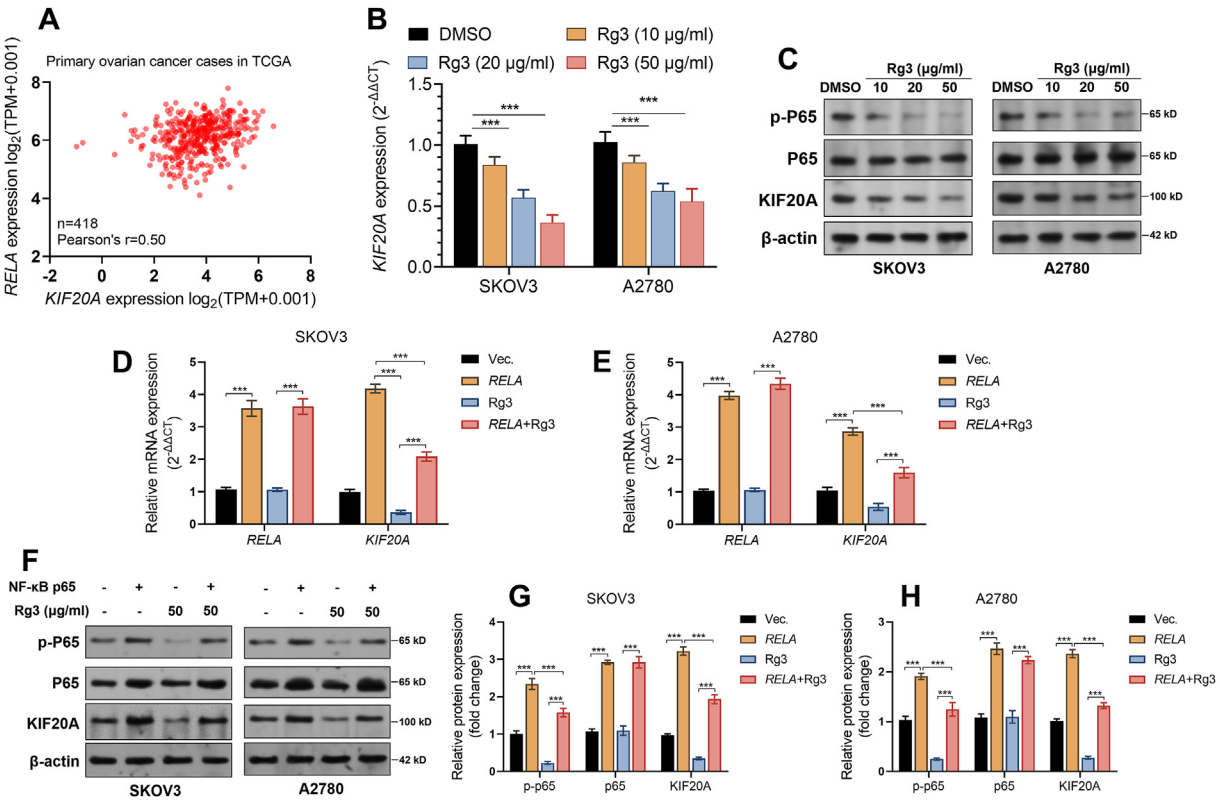

Fig. 3. Ginsenoside Rg3 suppresses *KIF20A* expression in ovarian cancer cells, **A.** A plot chart showing the expressional correlation between *KIF20A* and *RELA* in primary tumor cases in TCGA-OV. **B**–**C.** QRT-PCR (B) and western blotting assay (C) were performed to detect the expression of *KIF20A* in SKOV3 and A2780 cells 48 h after ginsenoside Rg3 treatment. **D-H.** QRT-PCR (D-E) and western blotting assay (F–H) were performed to detect the expression of *RELA* and *KIF20A* in SKOV3 and A2780 cells with *RELA* overexpression alone or in combination with ginsenoside Rg3 treatment (50 ng/ml for 48 h). ***$p < 0.001$.

$SCF^{\beta-TrCP-1}$ complex. To verify this hypothesis, we examined the expression of cell division cycle 25 A (CDC25A), a well-known $SCF^{\beta-TrCP-1}$ substrate [37] in SKOV3 cells. QRT-PCR assays confirmed that *KIF20A* knockdown or overexpression did not alter *CDC25A* transcription (S1 Fig. G-H). Western blotting data showed that *KIF20A* knockdown did not alter BTRC expression but reduced the expression of CDC25A (Fig. 5A, top panel). However, when MG132 was added, *KIF20A* knockdown could not induce CDC25A downregulation (Fig. 5A, bottom panel), suggesting that KIF20A might affect the proteasomal degradation of CDC25A. Therefore, we assessed the effect of KIF20A on $SCF^{\beta-TrCP-1}$ ubiquitin ligase activity for CDC25A. In brief, SKOV3 cells were infected with lentiviruses with selective overexpression of HA-ubiquitin (HA-Ub), Myc-BTRC, and/or flag-KIF20A (Fig. 5B). The ubiquitination of CDC25A was checked after IP using an anti-CDC25A antibody. The myc-BTRC group had a higher level of high molecular-weight smeared bands of CDC25A, indicating increased CDC25A poly-ubiquitination (Fig. 5B). *KIF20A* overexpression attenuated CDC25A poly-ubiquitination (Fig. 5B). In comparison, its knockdown increased CDC25A poly-ubiquitination (Fig. 5C). CHX chase assay showed that *KIF20A* overexpression increased the stability of CDC25A (Fig. 5D–E). *KIF20A* knockdown shortened the half-life of CDC25A (Fig. 5F–G).

Ginsenoside Rg3 treatment reduced CDC25A protein levels in a dose-dependent manner (Fig. 5H), the effect of which was canceled by adding MG132 (Fig. 5I). In addition, it partly abrogated *KIF20A* overexpression-induced CDC25A upregulation (Fig. 5J). These findings imply that ginsenoside Rg3 can promote CDC25A proteasomal degradation by suppressing *KIF20A* expression.

3.6. Ginsenoside Rg3 impairs ovarian tumor growth in vivo

To explore the regulatory effect of KIF20A on *in vivo* growth ovarian tumors, we generated xenograft tumor models in nude mice. Ovarian tumors derived from SKOV3 or A2780 cells with *KIF20A* knockdown grew significantly slower than those without *KIF20A* knockdown (Fig. 6A–D). CDC25A expression was also significantly lower in the group with KIF20A knockdown (Fig. 6F–G). IHC staining of Ki-67 confirmed that the tumors with *KIF20A* knockdown had fewer cells with positive Ki-67 staining (Fig. 6H). To validate the tumor suppressive effect of ginsenoside Rg3 *in vivo*, we generated xenograft tumor models in nude mice using SKOV3 cells with *KIF20A* overexpression. KIF20A overexpression significantly promoted tumor growth, accompanied by CDC25A upregulation (Fig. 6I–J). However, ginsenoside Rg3 treatment significantly retarded *KIF20A* overexpression-induced tumor growth and decreased CDC25A expression (Fig. 6I–J).

3.7. KIF20A expression was positively correlated with CDC25A expression in human epithelial ovarian cancer tissues

To validate the correlation between KIF20A and CDC25A expression, we used commercial tissue microarrays (continuous sections, Bioaitech, Xi'an, China), containing 59 human epithelial ovarian cancer cases. IHC staining and the following analysis of IHC scores by Spearman's correlation observed a moderate positive correlation between KIF20A and CDC25A in the 59 tumor tissue cases (Spearman's rho = 0.49, Fig. 7A–B).

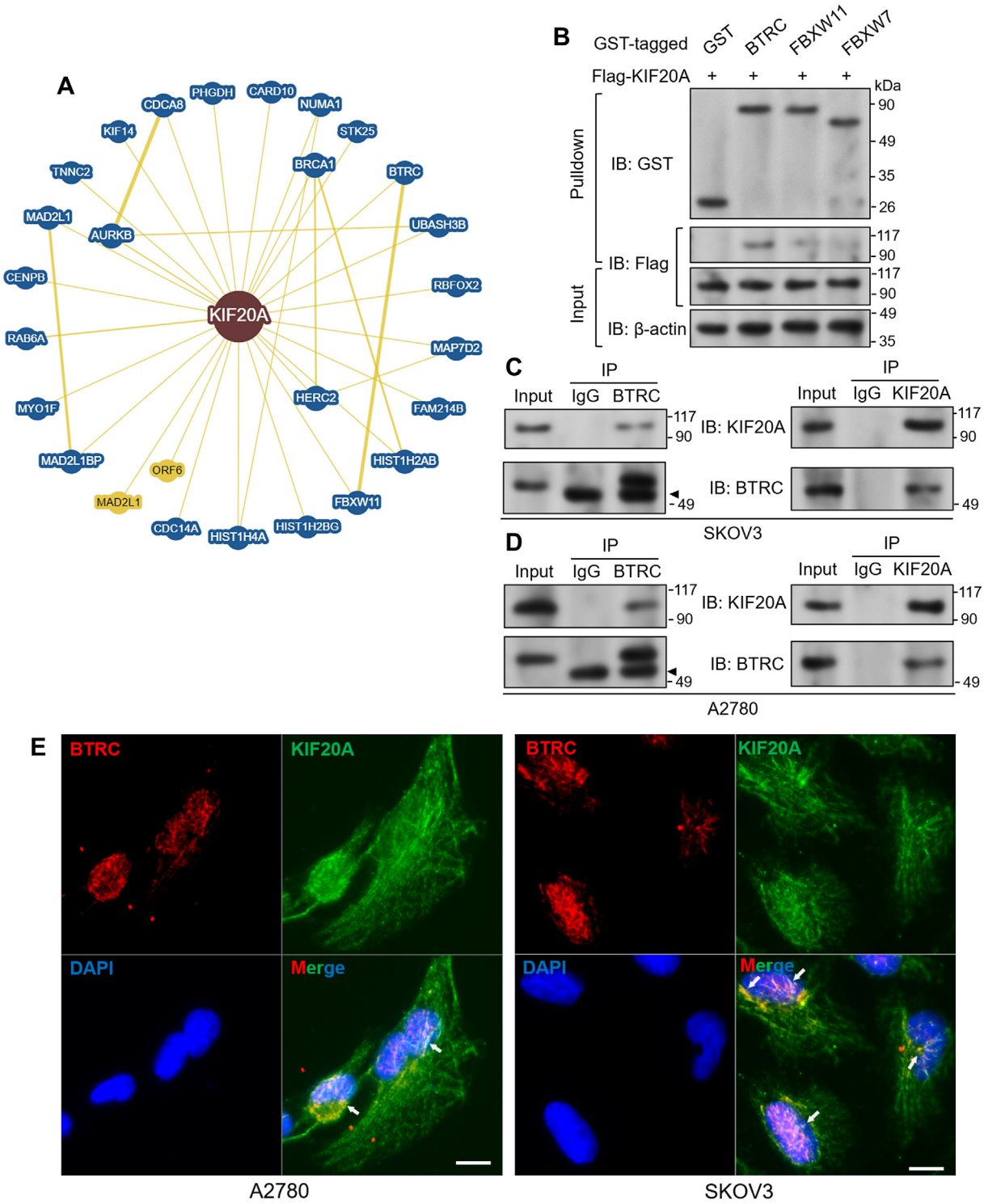

Fig. 4. KIF20A directly interacts with BTRC, **A.** Bioinformatic prediction of KIF20A interacting proteins. Prediction was performed using BioGRID. Only the proteins with minimum evidence ≥2 were identified as the candidates. **B.** Binding affinity of flag-KIF20A to the predicted E3 ligases. After various GST-fused proteins were expressed, a GST pull-down assay was performed. **C-D.** Co-IP was performed to show the interaction between KIF20A and BTRC at the endogenous level in SKOV3 (C) and A2780 (D) cells. IP was conducted with an anti-BTRC or anti-KIF20A antibody. Mouse IgG served as a negative control. Arrowheads: IgG heavy chain bands. **E.** Immunofluorescent staining was performed to visualize BTRC (red) and KIF20A (green) in SKOV3 and A2780 cells. Scale bar: 10 μm.

4. Discussion

Via bioinformatic analysis, we confirmed that *KIF20A* is significantly upregulated in ovarian cancer, and its upregulation is a biomarker of prognosis. The human KIF20A encodes a protein consisting of 890 amino acids. Aberrant *KIF20A* expression is associated with malignant behaviors and unfavorable clinical outcomes in multiple cancers [38–41], including ovarian cancer [24,25]. *KIF20A* was transcriptionally activated by FOXM1 in ovarian cancer and can promote the proliferation and invasion of ovarian

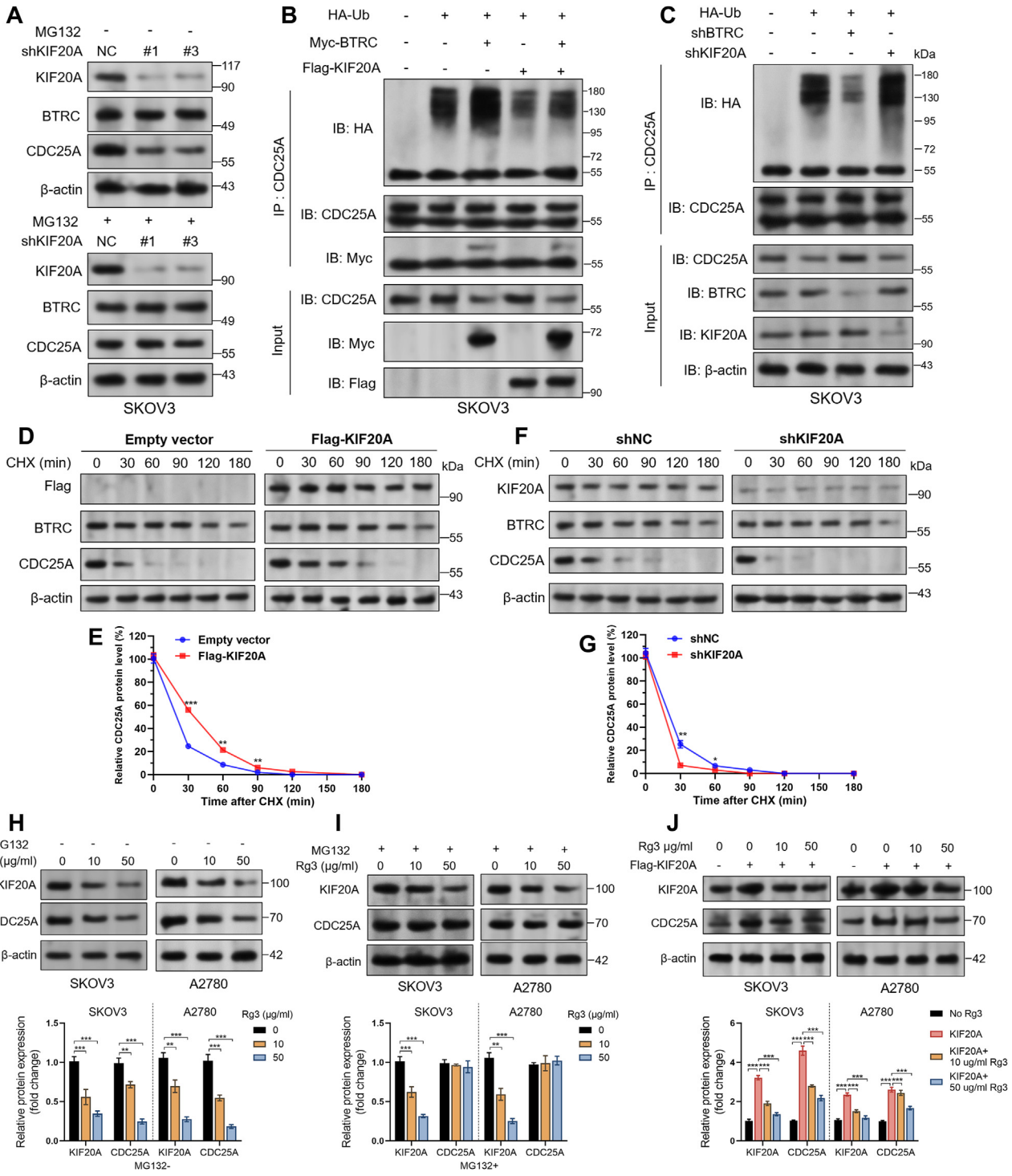

Fig. 5. Ginsenoside Rg3 promotes CDC25A proteasomal degradation via suppressing *KIF20A* expression, **A.** SKOV3 cells were subjected to lentiviral mediated *KIF20A* knockdown for 48 h, with or without the presence of MG132 (10 μM for 2 h before harvest). **B**–**C.** Western blot of *in vitro* ubiquitination assay. SKOV3 cells were infected with indicating selective combination of pLenti-puro-HA-Ubiquitin, myc-BTRC and/or flag-tagged KIF20A (B) or were infected with indicating selective combination of pLenti-puro-HA-Ubiquitin and shBTRC or shKIF20A (C). 48 h later, cells were lysed and the cell lysates were subjected to IP with an anti-CDC25A antibody. **D-G.** SKOV3 cells were infected for KIF20A overexpression (D-E) or knockdown (F-G). Then, the cells were incubated in the presence of 20 μM CHX for the indicated times (n = 3). Proteins were then analyzed by western blotting with the indicated antibodies. Relative levels of CDC25A (E and G) were determined from western blots using the ImageJ program based on the respective blots. **H**–**I.** Representative images (top panels) and quantitation (bottom panels) of western blotting analysis of KIF20A and CDC25A expression in SKOV3 and A2780 cells were subjected to ginsenoside Rg3 treatment for 48 h, with (I) or without (H) the presence of MG132 (10 μM for 2 h before harvest). **J.** SKOV3 and A2780 cells were subjected to lentiviral-mediated *KIF20A* knockdown. 48 h later, cells in indicated groups were treated with ginsenoside Rg3 for another 48 h. Then, cell samples were collected for western blotting analysis of KIF20A and CDC25A expression. Data are expressed as mean ± SD. Compared with the control group: $*p < 0.05$, $**p < 0.01$, $***p < 0.001$.

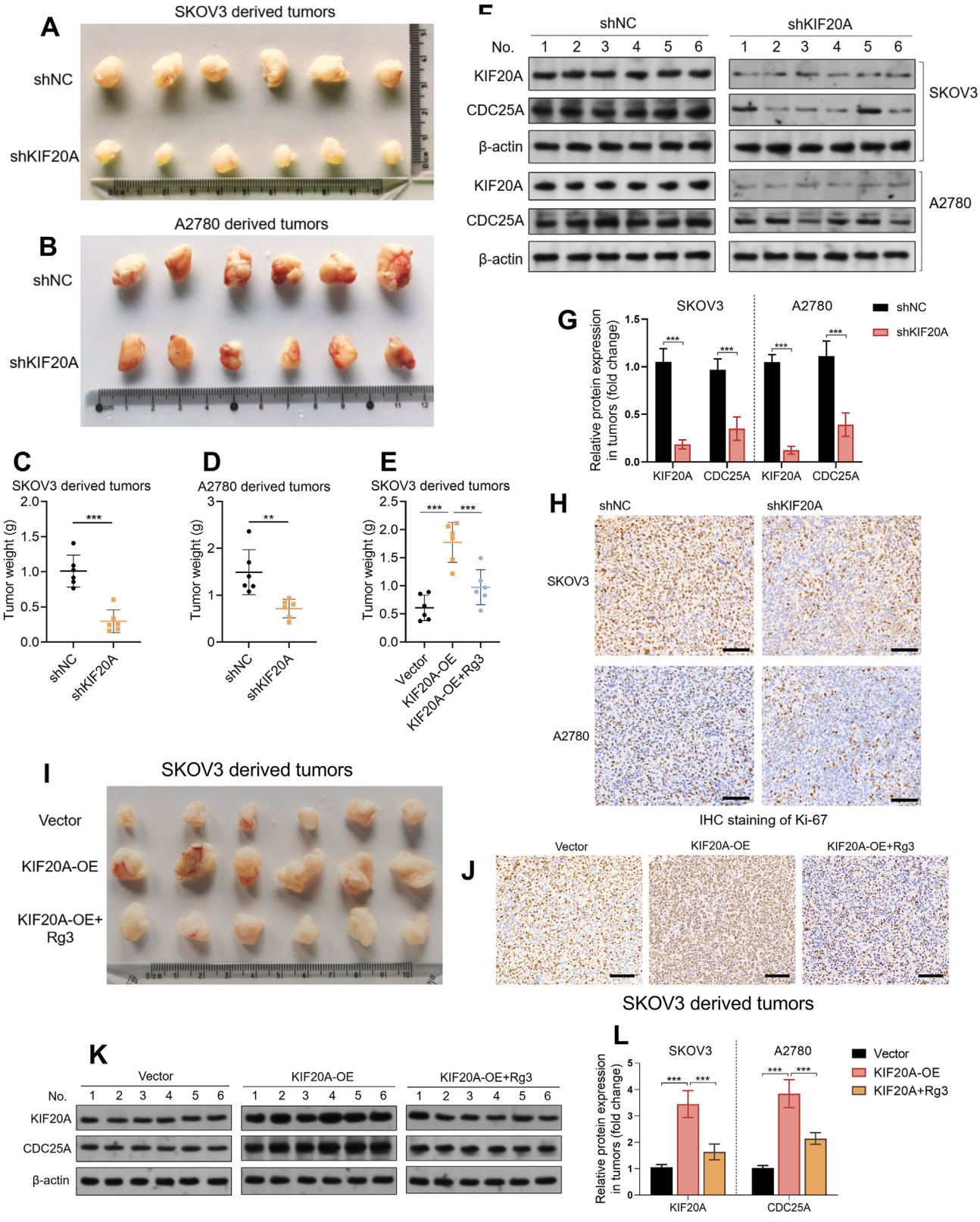

Fig. 6. The *in vivo* regulatory effect of KIF20A and its correlation with CDC25A in human epithelial ovarian cancer tissues, **A-D.** Xenograft tumors (A-D) and their weight (C-D), derived from SKOV3 (A) and A2780 (B) cells with or without *KIF20A* knockdown (n = 6). **F-G.** Representative images (F) and quantitation (G) of KIF20A and CDC25A proteins in tumor tissues in panel A, detected by western blotting. β-actin was used as a loading control. **H.** Representative images of immunohistochemical staining for Ki-67 in xenograft tumor tissues in panel A. **I and E.** Xenograft tumors (I) and their weight (E), derived from SKOV3 cells with *KIF20A* overexpression alone or in combination with ginsenoside Rg3 treatment (n = 6). **J.** Representative images of immunohistochemical staining for Ki-67 in xenograft tumor tissues in panel I. **K-L.** Representative images (K) and quantitation (L) of KIF20A and CDC25A proteins in tumor tissues in panel I, detected by western blotting. β-actin was used as a loading control. Data are expressed as mean ± SD. Compared with the control group: $^{**}p < 0.01$, $^{***}p < 0.001$. Panels H and J, scale bar: 100 μm.

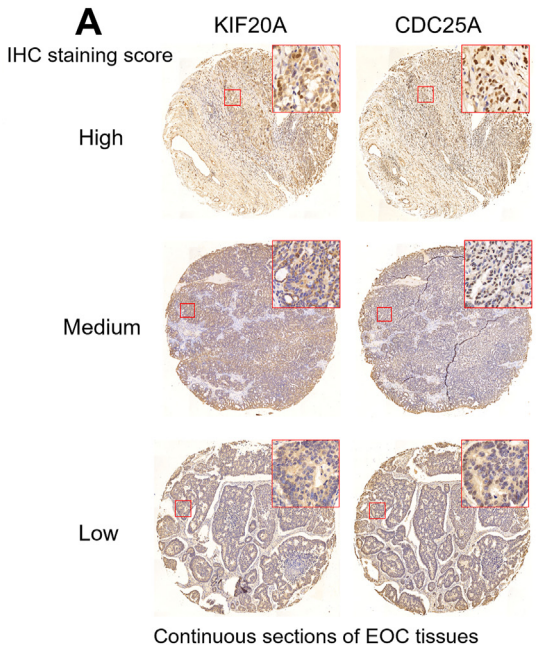

B

Correlation between the expression of KIF20A and CDC25A in EOC tissues

KIF20A staining score	CDC25A staining score				Total number
	Negative	Low	Medium	High	
Negative	0	1	0	0	1
Low	3	5	10	4	22
Medium	0	5	5	9	19
High	0	0	5	12	17
Total number	3	11	20	25	59

Spearman's rho=0.49

Fig. 7. The correlation between KIF20A and CDC25A expression in human epithelial ovarian cancer tissues, **A.** Representative IHC staining images of high, medium, and low KIF20A (left panel) and CDC25A (right panel) expression in two continuous ovarian cancer tissue microarrays (A). **B.** Correlation between KIF20A and CDC25A staining scores in 59 ovarian cancer tissues. Spearman's correlation analysis was conducted.

cancer cells [25]. In this study, using A2780 and SKOV3 cells as *in vitro* and *in vivo* cell models, we confirmed that the knockdown of *KIF20A* can significantly suppress tumor cell growth. These findings suggest that KIF20A might act as an important player in the pathological development of ovarian cancer.

KIF20A expression might be activated by NF-κB/P65, and ginsenoside Rg3 has confirmed effects on inhibiting the activity of P65 [32–34]. These clues suggest that ginsenoside Rg3 might suppress *KIF20A* expression. Our *in vitro* studies confirmed that ginsenoside Rg3 could inhibit the phosphorylation of P65 and transcription of *KIF20A*. Since ginsenoside Rg3 shows potent tumor-suppressive effects in ovarian cancer [15–18], we infer that KIF20A might be a downstream effector of ginsenoside Rg3.

KIF20A exerts biological regulations mainly via interacting with other molecules [42,43]. It interacts with the chromosomal passenger complex (CPC) and mediates localization in anaphase [44]. It interacts with the Regulator of G Protein Signaling 3 (RGS3) and controls the division modes of neural progenitor cells during cortical neurogenesis [45]. Therefore, the current study focused on its interacting proteins in ovarian cancer. By applying GST pull-down and co-IP assays, we found that it physically interacts with BTRC, a substrate recognition subunit for $SCF^{\beta-TrCP}$ E3 ubiquitin ligase. This protein can promote protein degradation by recognizing the phosphorylation of critical signaling molecules with crucial roles in cell cycle regulation, DNA damage response, and cancer progression [46,47]. $SCF^{\beta-TrCP}$ E3 ubiquitin ligase can recognize phosphorylated AEBP2 and target it for ubiquitylation and proteasomal degradation, leading to cisplatin resistance in ovarian cancer [48].

Among the substrates of $SCF^{\beta-TrCP}$ E3 ubiquitin ligase, CDC25A is a critical cell-cycle regulator, and its dysregulation is closely associated with chemoresistance in ovarian cancer [49]. CDC25A removes the inhibitory phosphorylation in cyclin-dependent kinase 4 (CDK4), CDK6, and CDK2 and promotes the cell-cycle progression during the G1/S and G2/M phases [50]. Inhibiting CDC25A using a small molecular inhibitor could sensitize ovarian cancer multicellular spheroids to chemotherapeutic agents [49]. The mechanisms underlying CDC25A upregulation are quite complex in cancer. Increased transcription, translation, and protein stability can elevate its expression in tumor cells. Some proteins can reduce CDC25A degradation via the ubiquitin-proteasome pathway via physical binding during cell cycle progression. For example, Rho-associated coiled-coil-containing protein kinase 2 (Rock2) can interact with CDC25A and reduce its ubiquitination and degradation in hepatocellular carcinoma cells [51]. CENPW can slow CDC25A degradation by interacting with and destabilizing the $SCF^{\beta-TrCP}$ complex during the G2/M phase [52]. Therefore, we further explored whether KIF20A affects the stability of CDC25A. By performing *in vitro* ubiquitination and CHX chase assays, we confirmed that via interacting with BTRC, KIF20A could reduce BTRC-mediated CDC25A poly-ubiquitination and enhance its stability. In addition, we confirmed that ginsenoside Rg3 treatment could reduce CDC25A protein levels and abrogate *KIF20A* overexpression-induced CDC25A upregulation in SKOV3 and A2780 cells. Therefore, we infer that ginsenoside Rg3 can promote CDC25A proteasomal degradation by suppressing *KIF20A* expression.

5. Conclusion

In summary, *KIF20A* is a tumor-promoting gene in ovarian cancer. KIF20A physically interacts with BTRC, reduces BTRC-mediated CDC25A poly-ubiquitination, and enhances its stability. Ginsenoside Rg3 can inhibit *KIF20A* transcription, thereby promoting CDC25A proteasomal degradation. These findings revealed a novel anti-tumor mechanism of ginsenoside Rg3 in ovarian cancer.

Funding

This study was supported by Tianjin Key Medical Discipline (Specialty) Construction Project (TJYXZDXK-031A), Natural Science Foundation of Shanxi Province (grant no.202103021223422 and

202203021221261), and in part, by the National Natural Science Foundation of China (grant nos. 82073264).

Data availability statements

All data generated or analyzed during this study are included in this published article.

Declaration of competing interest

The authors declare that they have no known competing financial interests or personal relationships that could have appeared to influence the work reported in this paper.

Appendix A. Supplementary data

Supplementary data to this article can be found online at https://doi.org/10.1016/j.jgr.2023.06.008.

References

[1] Shen L, Xia M, Zhang Y, Luo H, Dong D, Sun L. Mitochondrial integration and ovarian cancer chemotherapy resistance. Epub 2021/03/01 Exp Cell Res 2021;401(2):112549. https://doi.org/10.1016/j.yexcr.2021.112549. PubMed PMID: 33640393.

[2] Coughlan AY, Testa G. Exploiting epigenetic dependencies in ovarian cancer therapy. Epub 2021/07/03 Int J Cancer 2021;149(10):1732–43. https://doi.org/10.1002/ijc.33727. PubMed PMID: 34213777.

[3] Crean-Tate KK, Braley C, Dey G, Esakov E, Saygin C, Trestan A, et al. Pre-treatment with LCK inhibitors chemosensitizes cisplatin-resistant endometrioid ovarian tumors. Epub 2021/04/24 J Ovarian Res 2021;14(1):55. https://doi.org/10.1186/s13048-021-00797-x. PubMed PMID: 33888137; PubMed Central PMCID: PMCPMC8063392.

[4] Franzese E, Diana A, Centonze S, Pignata S, De Vita F, Ciardiello F, et al. PARP Inhibitors in First-Line Therapy of Ovarian Cancer: Are There Any Doubts?. Epub 2020/07/01 Front Oncol 2020;10:782. https://doi.org/10.3389/fonc.2020.00782. PubMed PMID: 32596142; PubMed Central PMCID: PMCPMC7303974.

[5] Bu H, Chen J, Li Q, Hou J, Wei Y, Yang X, et al. BRCA mutation frequency and clinical features of ovarian cancer patients: A report from a Chinese study group. Epub 2019/08/15 J Obstet Gynaecol Res 2019;45(11):2267–74. https://doi.org/10.1111/jog.14090. PubMed PMID: 31411802.

[6] Shi T, Wang P, Xie C, Yin S, Shi D, Wei C, et al. BRCA1 and BRCA2 mutations in ovarian cancer patients from China: ethnic-related mutations in BRCA1 associated with an increased risk of ovarian cancer. Epub 2017/02/09 Int J Cancer 2017;140(9):2051–9. https://doi.org/10.1002/ijc.30633. PubMed PMID: 28176296.

[7] Mikula-Pietrasik J, Witucka A, Pakula M, Uruski P, Begier-Krasinska B, Niklas A, et al. Comprehensive review on how platinum- and taxane-based chemotherapy of ovarian cancer affects biology of normal cells. Epub 2018/11/02 Cell Mol Life Sci 2019;76(4):681–97. https://doi.org/10.1007/s00018-018-2954-1. PubMed PMID: 30382284; PubMed Central PMCID: PMCPMC6514066.

[8] Hwang SK, Jeong YJ, Cho HJ, Park YY, Song KH, Chang YC. Rg3-enriched red ginseng extract promotes lung cancer cell apoptosis and mitophagy by ROS production. Epub 2022/01/22 J Ginseng Res 2022;46(1):138–46. https://doi.org/10.1016/j.jgr.2021.05.005. PubMed PMID: 35058730; PubMed Central PMCID: PMCPMC8753562.

[9] Lee A, Yun E, Chang W, Kim J. Ginsenoside Rg3 protects against iE-DAP-induced endothelial-to-mesenchymal transition by regulating the miR-139-5p-NF-kappaB axis. Epub 2020/03/10 J Ginseng Res 2020;44(2):300–7. https://doi.org/10.1016/j.jgr.2019.01.003. PubMed PMID: 32148412; PubMed Central PMCID: PMCPMC7031736.

[10] Pan H, Yang L, Bai H, Luo J, Deng Y. Ginsenoside Rg3 increases gemcitabine sensitivity of pancreatic adenocarcinoma via reducing ZFP91 mediated TSPYL2 destabilization. Epub 2022/09/13 J Ginseng Res 2022;46(5):636–45. https://doi.org/10.1016/j.jgr.2021.08.004. PubMed PMID: 36090681; PubMed Central PMCID: PMCPMC9459078.

[11] Park EH, Kim YJ, Yamabe N, Park SH, Kim HK, Jang HJ, et al. Stereospecific anticancer effects of ginsenoside Rg3 epimers isolated from heat-processed American ginseng on human gastric cancer cell. Epub 2014/02/22 J Ginseng Res 2014;38(1):22–7. https://doi.org/10.1016/j.jgr.2013.11.007. PubMed PMID: 24558306; PubMed Central PMCID: PMCPMC3915326.

[12] Yuan Z, Jiang H, Zhu X, Liu X, Li J. Ginsenoside Rg3 promotes cytotoxicity of Paclitaxel through inhibiting NF-kappaB signaling and regulating Bax/Bcl-2 expression on triple-negative breast cancer. Epub 2017/02/24 Biomed Pharmacother 2017;89:227–32. https://doi.org/10.1016/j.biopha.2017.02.038. PubMed PMID: 28231544.

[13] Zhao L, Shou H, Chen L, Gao W, Fang C, Zhang P. Effects of ginsenoside Rg3 on epigenetic modification in ovarian cancer cells. Epub 2019/04/20 Oncol Rep 2019;41(6):3209–18. https://doi.org/10.3892/or.2019.7115. PubMed PMID: 31002353; PubMed Central PMCID: PMCPMC6489025.

[14] Park JY, Choi P, Lee D, Kim T, Jung EB, Hwang BS, et al. Effect of Amino Acids on the Generation of Ginsenoside Rg3 Epimers by Heat Processing and the Anticancer Activities of Epimers in A2780 Human Ovarian Cancer Cells. Epub 2016/04/07 Evid Based Complement Alternat Med 2016;2016:3146402. https://doi.org/10.1155/2016/3146402. PubMed PMID: 27051448; PubMed Central PMCID: PMCPMC4804038.

[15] Liu T, Zhao L, Zhang Y, Chen W, Liu D, Hou H, et al. Ginsenoside 20(S)-Rg3 targets HIF-1alpha to block hypoxia-induced epithelial-mesenchymal transition in ovarian cancer cells. Epub 2014/09/10 PLoS ONE 2014;9(9):e103887. https://doi.org/10.1371/journal.pone.0103887. PubMed PMID: 25197976; PubMed Central PMCID: PMCPMC4157750.

[16] Zheng X, Chen W, Hou H, Li J, Li H, Sun X, et al. Ginsenoside 20(S)-Rg3 induced autophagy to inhibit migration and invasion of ovarian cancer. Epub 2016/12/03 Biomed Pharmacother 2017;85:620–6. https://doi.org/10.1016/j.biopha.2016.11.072. PubMed PMID: 27899249.

[17] Lu J, Chen H, He F, You Y, Feng Z, Chen W, et al. Ginsenoside 20(S)-Rg3 upregulates HIF-1alpha-targeting miR-519a-5p to inhibit the Warburg effect in ovarian cancer cells. Epub 2020/04/10 Clin Exp Pharmacol Physiol 2020;47(8):1455–63. https://doi.org/10.1111/1440-1681.13321. PubMed PMID: 32271958.

[18] Zhao L, Sun W, Zheng A, Zhang Y, Fang C, Zhang P. Ginsenoside Rg3 suppresses ovarian cancer cell proliferation and invasion by inhibiting the expression of lncRNA H19. Epub 2021/05/27 Acta Biochim Pol 2021;68(4):575–82. https://doi.org/10.18388/abp.2020_5343. PubMed PMID: 34038042.

[19] Zhong A, Tan FQ, Yang WX. Chromokinesin: kinesin superfamily regulating cell division through chromosome and spindle. Epub 2016/05/20 Gene 2016;589(1):43–8. https://doi.org/10.1016/j.gene.2016.05.026. PubMed PMID: 27196062.

[20] Liu X, Gong H, Huang K. Oncogenic role of kinesin proteins and targeting kinesin therapy. Epub 2013/02/27 Cancer Sci 2013;104(6):651–6. https://doi.org/10.1111/cas.12138. PubMed PMID: 23438337; PubMed Central PMCID: PMCPMC7657121.

[21] Lucanus AJ, Yip GW. Kinesin superfamily: roles in breast cancer, patient prognosis and therapeutics. Epub 2017/10/24 Oncogene 2018;37(7):833–8. https://doi.org/10.1038/onc.2017.406. PubMed PMID: 29059174.

[22] Theriault BL, Pajovic S, Bernardini MQ, Shaw PA, Gallie BL. Kinesin family member 14: an independent prognostic marker and potential therapeutic target for ovarian cancer. Epub 2011/05/28 Int J Cancer 2012;130(8):1844–54. https://doi.org/10.1002/ijc.26189. PubMed PMID: 21618518.

[23] Yamamoto J, Amishiro N, Kato K, Ohta Y, Ino Y, Araki M, et al. Synthetic studies on mitotic kinesin Eg5 inhibitors: synthesis and structure-activity relationships of novel 2,4,5-substituted-1,3,4-thiadiazoline derivatives. Epub 2014/07/09 Bioorg Med Chem Lett 2014;24(16):3961–3. https://doi.org/10.1016/j.bmcl.2014.06.034. PubMed PMID: 25001485.

[24] Li H, Zhang W, Sun X, Chen J, Li Y, Niu C, et al. Overexpression of kinesin family member 20A is associated with unfavorable clinical outcome and tumor progression in epithelial ovarian cancer. Epub 2018/09/27 Cancer Manag Res 2018;10:3433–50. https://doi.org/10.2147/CMAR.S169214. PubMed PMID: 30254487; PubMed Central PMCID: PMCPMC6140728.

[25] Li Y, Guo H, Wang Z, Bu H, Wang S, Wang H, et al. Cyclin F and KIF20A, FOXM1 target genes, increase proliferation and invasion of ovarian cancer cells. Epub 2020/08/11 Exp Cell Res 2020;395(2):112212. https://doi.org/10.1016/j.yexcr.2020.112212. PubMed PMID: 32771525.

[26] Goldman MJ, Craft B, Hastie M, Repecka K, McDade F, Kamath A, et al. Visualizing and interpreting cancer genomics data via the Xena platform. Epub 2020/05/24 Nat Biotechnol 2020;38(6):675–8. https://doi.org/10.1038/s41587-020-0546-8. PubMed PMID: 32444850.

[27] Uhlen M, Oksvold P, Fagerberg L, Lundberg E, Jonasson K, Forsberg M, et al. Towards a knowledge-based human protein atlas. Epub 2010/12/09 Nat Biotechnol 2010;28(12):1248–50. https://doi.org/10.1038/nbt1210-1248. PubMed PMID: 21139605.

[28] Gyorffy B, Lanczky A, Szallasi Z. Implementing an online tool for genome-wide validation of survival-associated biomarkers in ovarian-cancer using microarray data from 1287 patients. Epub 2012/01/27 Endocr Relat Cancer 2012;19(2):197–208. https://doi.org/10.1530/ERC-11-0329. PubMed PMID: 22277193.

[29] Garrido MP, Hurtado I, Valenzuela-Valderrama M, Salvatierra R, Hernandez A, Vega M, et al. NGF-Enhanced Vasculogenic Properties of Epithelial Ovarian Cancer Cells Is Reduced by Inhibition of the COX-2/PGE2 Signaling Axis. Epub 2019/12/11 Cancers (Basel) 2019;11(12). https://doi.org/10.3390/cancers11121970. PubMed PMID: 31817839; PubMed Central PMCID: PMCPMC6966471.

[30] Zhang R, Li L, Chen L, Suo Y, Fan J, Zhang S, et al. MAP7 interacts with RC3H1 and cooperatively regulate cell-cycle progression of cervical cancer cells via activating the NF-kappaB signaling. Epub 2020/05/25 Biochem Biophys Res Commun 2020;527(1):56–63. https://doi.org/10.1016/j.bbrc.2020.04.008. PubMed PMID: 32446391.

[31] Donaldson JG. Immunofluorescence staining. Epub 2015/12/02 Curr Protoc Cell Biol 2015;69(3 7):4 3 1–4. https://doi.org/10.1002/0471143030.cb0403s69. PubMed PMID: 26621373.

[32] Kim BM, Kim DH, Park JH, Surh YJ, Na HK. Ginsenoside Rg3 inhibits constitutive activation of NF-kappaB signaling in human breast cancer (MDA-MB-231) cells: ERK and akt as potential upstream targets. Epub 2014/10/23 J Cancer Prev 2014;19(1):23–30. https://doi.org/10.15430/jcp.2014.19.1.23. PubMed PMID: 25337569; PubMed Central PMCID: PMCPMC4189477.

[33] Shan X, Tian LL, Zhang YM, Wang XQ, Yan Q, Liu JW. Ginsenoside Rg3 suppresses FUT4 expression through inhibiting NF-kappaB/p65 signaling pathway to promote melanoma cell death. Epub 2015/06/23 Int J Oncol 2015;47(2):701–9. https://doi.org/10.3892/ijo.2015.3057. PubMed PMID: 26094873; PubMed Central PMCID: PMCPMC6903900.

[34] Tu C, Wan B, Zeng Y. Ginsenoside Rg3 alleviates inflammation in a rat model of myocardial infarction via the SIRT1/NF-kappaB pathway. Epub 2020/11/17 Exp Ther Med 2020;20(6):238. https://doi.org/10.3892/etm.2020.9368. PubMed PMID: 33193843; PubMed Central PMCID: PMCPMC7646702.

[35] Fuchs SY, Spiegelman VS, Kumar KG. The many faces of beta-TrCP E3 ubiquitin ligases: reflections in the magic mirror of cancer. Epub 2004/03/17 Oncogene 2004;23(11):2028–36. https://doi.org/10.1038/sj.onc.1207389. PubMed PMID: 15021890.

[36] Bi Y, Cui D, Xiong X, Zhao Y. The characteristics and roles of beta-TrCP1/2 in carcinogenesis. Epub 2020/10/07 FEBS J 2021;288(11):3351–74. https://doi.org/10.1111/febs.15585. PubMed PMID: 33021036.

[37] Busino L, Donzelli M, Chiesa M, Guardavaccaro D, Ganoth D, Dorrello NV, et al. Degradation of Cdc25A by beta-TrCP during S phase and in response to DNA damage. Epub 2003/11/07 Nature 2003;426(6962):87–91. https://doi.org/10.1038/nature02082. PubMed PMID: 14603323.

[38] Zhang Z, Chai C, Shen T, Li X, Ji J, Li C, et al. Aberrant KIF20A Expression Is Associated with Adverse Clinical Outcome and Promotes Tumor Progression in Prostate Cancer. Epub 2019/10/01 Dis Markers 2019;2019:4782730. https://doi.org/10.1155/2019/4782730. PubMed PMID: 31565099; PubMed Central PMCID: PMCPMC6745134.

[39] Copello VA, Burnstein KL. The kinesin KIF20A promotes progression to castration-resistant prostate cancer through autocrine activation of the androgen receptor. Epub 2022/04/15 Oncogene 2022. https://doi.org/10.1038/s41388-022-02307-9. PubMed PMID: 35418689.

[40] Xiong M, Zhuang K, Luo Y, Lai Q, Luo X, Fang Y, et al. KIF20A promotes cellular malignant behavior and enhances resistance to chemotherapy in colorectal cancer through regulation of the JAK/STAT3 signaling pathway. Epub 2019/12/17 Aging 2019;11(24):11905–21. https://doi.org/10.18632/aging.102505. PubMed PMID: 31841120; PubMed Central PMCID: PMCPMC6949076.

[41] Lu M, Huang X, Chen Y, Fu Y, Xu C, Xiang W, et al. Aberrant KIF20A expression might independently predict poor overall survival and recurrence-free survival of hepatocellular carcinoma. Epub 2018/03/04 IUBMB Life 2018;70(4):328–35. https://doi.org/10.1002/iub.1726. PubMed PMID: 29500859.

[42] Qiu R, Runxiang Q, Geng A, Liu J, Xu CW, Menon MB, et al. SEPT7 Interacts with KIF20A and Regulates the Proliferative State of Neural Progenitor Cells During Cortical Development. Epub 2019/12/10 Cereb Cortex 2020;30(5):3030–43. https://doi.org/10.1093/cercor/bhz292. PubMed PMID: 31813992; PubMed Central PMCID: PMCPMC7197076.

[43] Wu WD, Yu KW, Zhong N, Xiao Y, She ZY. Roles and mechanisms of Kinesin-6 KIF20A in spindle organization during cell division. Epub 2018/12/24 Eur J Cell Biol 2019;98(2–4):74–80. https://doi.org/10.1016/j.ejcb.2018.12.002. PubMed PMID: 30579662.

[44] Adriaans IE, Hooikaas PJ, Aher A, Vromans MJM, van Es RM, Grigoriev I, et al. MKLP2 Is a Motile Kinesin that Transports the Chromosomal Passenger Complex during Anaphase. Epub 2020/06/06 Curr Biol 2020;30(13):2628–37. https://doi.org/10.1016/j.cub.2020.04.081. PubMed PMID: 32502404.

[45] Geng A, Qiu R, Murai K, Liu J, Wu X, Zhang H, et al. KIF20A/MKLP2 regulates the division modes of neural progenitor cells during cortical development. Epub 2018/07/15 Nat Commun 2018;9(1):2707. https://doi.org/10.1038/s41467-018-05152-1. PubMed PMID: 30006548; PubMed Central PMCID: PMCPMC6045631.

[46] Skaar JR, Pagan JK, Pagano M. SCF ubiquitin ligase-targeted therapies. Epub 2014/11/15 Nat Rev Drug Discov 2014;13(12):889–903. https://doi.org/10.1038/nrd4432. PubMed PMID: 25394868; PubMed Central PMCID: PMCPMC4410837.

[47] Lee EK, Diehl JA. SCFs in the new millennium. Epub 2013/04/30 Oncogene 2014;33(16):2011–8. https://doi.org/10.1038/onc.2013.144. PubMed PMID: 23624913.

[48] Zhang Q, Wang W, Gao Q. beta-TRCP-mediated AEBP2 ubiquitination and destruction controls cisplatin resistance in ovarian cancer. Epub 2019/12/23 Biochem Biophys Res Commun 2020;523(1):274–9. https://doi.org/10.1016/j.bbrc.2019.12.050. PubMed PMID: 31864706.

[49] Sun Y, Li S, Yang L, Zhang D, Zhao Z, Gao J, et al. CDC25A Facilitates Chemoresistance in Ovarian Cancer Multicellular Spheroids by Promoting E-cadherin Expression and Arresting Cell Cycles. Epub 2019/07/10 J Cancer 2019;10(13):2874–84. https://doi.org/10.7150/jca.31329. PubMed PMID: 31281464; PubMed Central PMCID: PMCPMC6590049.

[50] Shen T, Huang S. The role of Cdc25A in the regulation of cell proliferation and apoptosis. Epub 2012/01/24 Anticancer Agents Med Chem 2012;12(6):631–9. https://doi.org/10.2174/187152012800617678. PubMed PMID: 22263797; PubMed Central PMCID: PMCPMC3544488.

[51] Liu T, Yu X, Li G, Yuan R, Wang Q, Tang P, et al. Rock2 regulates Cdc25A through ubiquitin proteasome system in hepatocellular carcinoma cells. Epub 2012/06/19 Exp Cell Res 2012;318(16):1994–2003. https://doi.org/10.1016/j.yexcr.2012.04.017. PubMed PMID: 22705122.

[52] Cheon Y, Lee S. CENP-W inhibits CDC25A degradation by destabilizing the SCF(beta-TrCP-1) complex at G2/M. fj201701358RRR. Epub 2018/06/05 FASEB J 2018. https://doi.org/10.1096/fj.201701358RRR. PubMed PMID: 29863914.